International Journal of Multidisciplinary Research and Growth Evaluation.

Development of Advanced Biofuels from Agricultural Lignocellulosic Residues for Power Generation through Solar Photocatalytic Reactors

Ogbonna Bartholomew Odinaka [1*], Chizindu Stanley Esobinenwu [2]
[1-2] (PhD), Department of Electrical/Electronic Engineering, Faculty of Engineering, University of Port Harcourt, Choba, Rivers State, Nigeria

* Corresponding Author: **Ogbonna Bartholomew Odinaka**

Article Info
ISSN (online): 2582-7138
Volume: 06
Issue: 02
March-April 2025
Received: 14-02-2025
Accepted: 09-03-2025
Page No: 954-964

Abstract
This study investigated the development of advanced biofuels from agricultural lignocellulosic residues for power generation using solar photocatalytic reactors (SPRs). A simulation-based approach was adopted to optimize reactor design and operating conditions to achieve a biofuel conversion efficiency (η) ≥ 80% and purity (σ) ≥ 85%. The study evaluated the impact of temperature, pressure, and catalyst loading on biofuel yield, targeting an optimal range of 1.8-3.4 kWh/kg. A five-step methodology was employed, including feedstock characterization, reactor design, catalyst selection, computational fluid dynamics (CFD) and electrical power yield estimation. Various reactor types, sizes, and materials were analyzed, with findings indicating that a steel-based batch reactor with an optimal temperature of 378K maximized photon absorption and catalytic activation. Reactor size (A ≈ 3.8 m²) was determined to be ideal for minimizing energy losses while maintaining high purity. Pressure was identified as a key optimization factor, with 10 atm yielding the highest biofuel output (~2.784 kWh/kg). Catalyst loading at 0.1 g/L further enhanced the efficiency of semiconductor photocatalysts, with TiO_2, ZnO, and CdS exhibiting bandgap energies between 2.4-3.3 eV and quantum efficiencies of up to 90%. The solar absorption power was recorded at 1200W, with net electrical output estimated at 1038W after energy loss considerations. Findings challenged conventional temperature-dependent models, indicating that pressure compensated for lower temperatures. This research provided a framework for optimizing SPRs in biofuel production, emphasizing reactor material selection, fluid dynamics, and energy efficiency.

DOI: https://doi.org/10.54660/.IJMRGE.2025.6.2.954-964

Keywords: Solar Photocatalytic Reactors, Biofuel Conversion, Agricultural Lignocellulosic Residues, Catalyst Optimization, Power Generatio

Introduction

In sustainable energy engineering, Solar Photocatalytic Reactors (SPRs) represent a groundbreaking method for converting agricultural lignocellulosic residues into biofuels. These controlled photochemical systems employ semiconductor catalysts such as titanium dioxide (TiO_2), zinc oxide (ZnO), or cadmium sulfide (CdS) to drive photo-induced redox reactions under specific electromagnetic wavelengths. The fundamental mechanism involves electron-hole pair excitation within the photocatalyst's conduction and valence bands, thereby initiating oxidation-reduction reactions that decompose complex organic substrates into usable biofuels (Liu *et al*., 2019) [11]. The historical emergence of SPRs can be traced back to the pioneering photocatalytic water splitting experiments of the 1970s, which demonstrated the feasibility of decomposing water into hydrogen and oxygen using TiO_2 electrodes (Puga, 2016) [17].

Additionally, the integration of SPRs with agricultural waste valorization capitalizes on efficient photonic-electron excitation dynamics, ensuring higher energy conversion efficiency compared to conventional combustion or anaerobic digestion methods (Naveen *et al*., 2023) [14]. Unlike conventional combustion or anaerobic digestion processes, SPRs harness optical excitation energy rather than pure thermal energy, ensuring a higher energy conversion efficiency (ECE) given by the equation:

$$\eta ECE = \frac{P\_photonic\ input}{P\_electrical\ output} x100\%$$

Where
$P_{electrical\ output}$ = Actual electric power generated from the biofuel,
$P_{photonic\ input}$ = Incident solar energy absorbed by the catalytic material.

A higher ηECE value enhances SPR-based power generation, enabling scalable energy densities comparable to mid-tier bioethanol and biodiesel systems. When applied to agricultural biowaste like rice husk and sugarcane bagasse, SPRs can yield 1.8-3.4 kWh/kg of electrical energy, providing a viable alternative to thermal gasification (Ghalta *et al*., 2024) [8]. The efficiency of SPR-derived power depends on photocatalyst bandgap energy, quantum efficiency, and biomass composition. Additionally, SPR-based power generation ensures stable voltage regulation, high power factor correction, and minimal transient losses, outperforming combustion-based bioenergy systems in electrical performance (Velvizhi *et al*., 2022) [23]. The governing equation for power yield estimation in SPR-driven biofuel combustion engines follows:

$$P_{biofuel} = \eta_{comb} \cdot \left(\frac{\Delta H_{\text{biofuel}}}{M_{\text{biofuel}}} \right) \cdot m_{biofuel}$$

Where
η_{comb} = Thermal-to-electricity conversion efficiency,
$\Delta H_{biofuel}$ = Enthalpy of combustion per mole of biofuel,
$M_{biofuel}$ = Molecular weight,
$m_{biofuel}$ = Mass flow rate of the biofuel utilized.

The given equation underscores how SPR-synthesized biofuels exhibit controlled calorific values comparable to standardized fuel cells, facilitating their integration into hybrid photovoltaic-electrochemical microgrid architectures (Chen *et al*., 2023) [5]. However, not all agricultural waste is suitable for SPR processing, as feedstock selection depends on molecular heterogeneity, lignin-to-cellulose ratio, and catalytic degradation kinetics. Biowastes with high aromatic polymeric structures, such as hardwood lignin residues or seed husks with silica reinforcements, exhibit low photocatalytic degradation coefficients (k_d), leading to suboptimal hydrocarbon release rates (Mujtaba *et al*., 2023) [12]. Conversely, residues rich in hemicellulose, such as corn cobs or wheat straw, generate reactive volatile bio-oil intermediates that enhance SPR-driven pyrolytic conversion. SPR-compatible agricultural residues are classified based on dielectric permittivity (ε_r) and bio-oil conductivity (σ_{bio}), where ε_r governs charge transport efficiency, and σ_{bio} influences plasma arc ignition in direct biofuel combustion turbines (Rani *et al*., 2023) [18]. The empirical correlation governing these parameters is given by the charge displacement equation:

$$\vec{D} = \varepsilon_0 \varepsilon_r \vec{E}$$

Where
$\vec{D}$ = Electric displacement field,
ε_0 = Permittivity of free space,
$\vec{E}$ = Applied electric field within the reactor chamber.

High-ε_r biofuels enhance ionic charge mobility, reducing ohmic resistance and improving thermal-electrical conversion in SPRs with thermionic power cycles (Liu *et al*., 2019) [11]. SPR biofuel production remains semi-empirical, optimized via quantum dot modifications and multi-junction photocatalysts (Shi *et al*., 2023) [21]. Mathematical models predict power yields comparable to biomass cogeneration (Naveen *et al*., 2023) [14], Thus, this study embarked on valorizing agricultural lignocellulosic residues to derive EN 590-grade biofuels with η = 75-85% efficiency and σ = 80-≤90% purity for power generation through solar photocatalytic reactors.

Statement of the problem

Sub-Saharan Africa's severe energy crisis is marked by inadequate access to reliable, sustainable energy sources, perpetuating energy poverty and hindering economic growth. The region's fossil fuel reliance worsens climate change, while traditional biomass methods are inefficient and hardly sustainable. More so, agricultural activities generate massive lignocellulosic waste, polluting the environment through uncontrolled burning and decomposition. This waste can be harnessed for power generation, offering a cost-effective, environmentally friendly solution to the energy crisis, motivating this study to explore this sustainable alternative.

Aim and objectives of the study

This study was aimed at developing advanced biofuels from agricultural lignocellulosic residues for power generation through solar photocatalytic reactors. Specifically, the objectives were to:

1. Design and simulate a solar photocatalytic reactor system to achieve a biofuel conversion efficiency of $\eta \geq$ 80% and a purity of $\sigma \geq$ 85%.; and,
2. Simulate the optimal operating conditions (temperature, pressure, and catalyst loading) for solar photocatalytic reforming of lignocellulosic residues to achieve a minimum biofuel yield of 1.8-3.4 kWh/kg

Research Questions

1. What is the optimal reactor design configuration (reactor type, size, and material) for achieving a biofuel conversion efficiency of $\eta \geq$ 80% and a purity of $\sigma \geq$ 85%
2. What are the optimal operating conditions (temperature, pressure, and catalyst loading) for solar photocatalytic reforming of lignocellulosic residues to achieve a minimum biofuel yield of 1.8-3.4 kWh/kg?

Conceptual Framework

The concept of the study is based on advanced biofuels from agricultural lignocellulosic residues for power generation through solar photocatalytic reactors. This is represented in Figure 1.

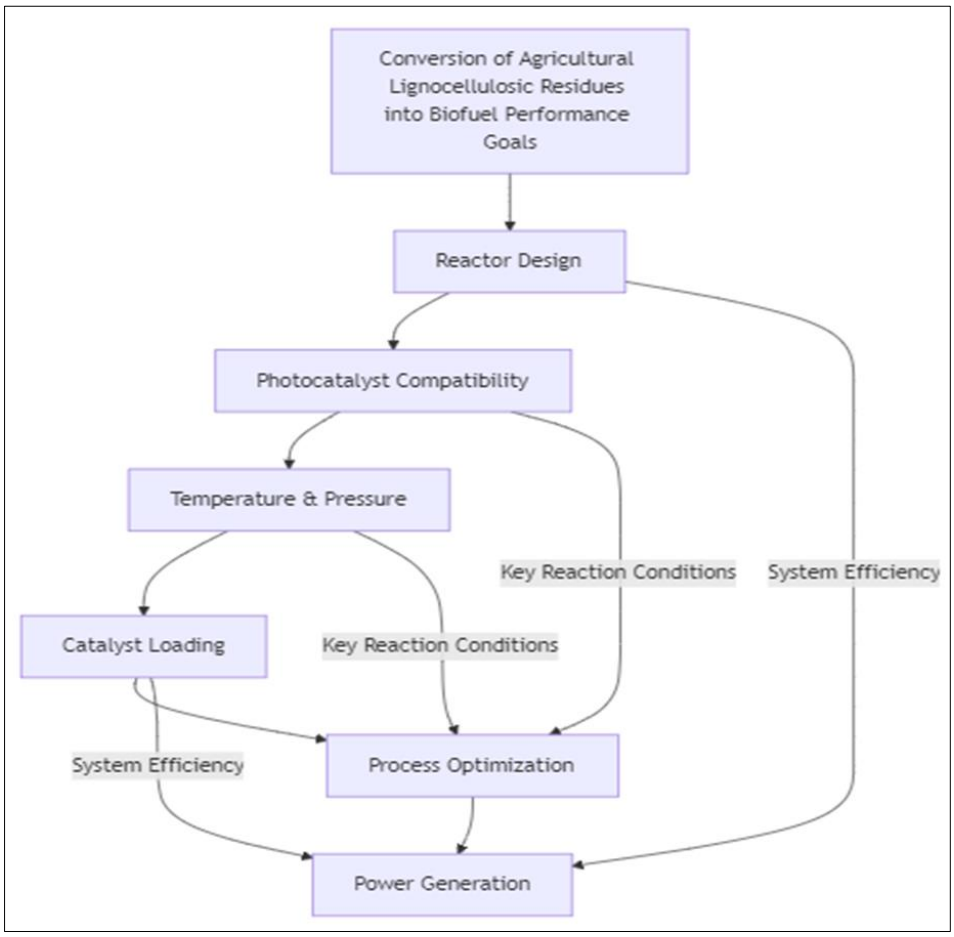

Source: Researchers' Conceptualizatiion (2025)

Fig 1: Showing the representation of the study's conceptual framework.

Literature Review

The growing energy crisis coupled with rapid population growth in sub-Saharan Africa has intensified the need for sustainable power solutions, with solar photocatalytic reactors (SPRs) emerging as key systems for biofuel generation. According to Aboagye *et al*. (2023) [1], these reactors leverage a photochemical system to drive photo-driven redox reactions, decomposing complex organic substrates into valuable fuels. More so, Mujtaba *et al*. (2023) [12] observed that the integration of titanium dioxide (TiO_2) and zinc oxide (ZnO) as photocatalysts within the reactor chamber enhances oxidation-reduction reactions by exploiting specific wavelengths within the electromagnetic spectrum. In tandem with this, Ghalta *et al*. (2024) [8] acknowledged that the applied electric field plays a critical role in modulating the photocatalyst's conduction band (CB) and valence band (VB), significantly improving charge separation and boosting higher energy conversion efficiency (ECE). As corroborated by Shi *et al*. (2023) [21] and Naveen *et al*. (2023) [14], multi-junction photocatalyst layering further enhances the reaction kinetics, allowing for a more effective thermochemical biofuel generation process. Additionally, Alazaiza *et al*. (2025) [2] admitted that the mass flow rate of biofuel utilized directly impacts the electric power generated from the biofuel, making precise reactor design and optimization essential. According to Puga (2016) [17], these factors play a significant role in ensuring energy-efficient biofuel production, which is also supported by Wu *et al*. (2018) [24].

A key factor in maximizing SPR efficiency is power factor correction, which, as noted by Velvizhi *et al*. (2022) [23], stabilizes the electric displacement field and ensures low ohmic resistance, enhancing thermal-electrical conversion. Furthermore, Reshmy *et al*. (2022) [19] and Rani *et al*. (2023) [18] observed that quantum dots contribute to increased photocatalyst efficiency and expanded absorption across specific wavelengths. More so, Naveen *et al*. (2023) [14] emphasized that integrating power factor correction with applied electric field adjustments leads to improved ECE, as corroborated by Shi *et al*. (2023) [20] and Sun *et al*. (2025) [22]. Moreover, Liu *et al*. (2019) [11] admitted that the enthalpy of combustion per mole of biofuel and molecular weight considerations are critical in optimizing biofuel performance. The combination of mathematical models and advanced reactor materials contributes to the precise control of reaction parameters, further enhancing decomposition efficiency (Deymi *et al*., 2025; Velvizhi *et al*., 2022; Jatoi *et al*., 2021; Okolie *et al*., 2021; Nasseh *et al*., 2020) [6, 23, 10, 16, 13]. High-ε_r biofuels have demonstrated superior energy yield, reducing system inefficiencies and supporting the expansion of biofuel-based energy grids (Sun *et al*., 2025; Shi *et al*., 2023; Liu *et al*., 2019) [22, 21, 11]. In line with these advancements, integrating applied electric field enhancements, thermal-electrical conversion improvements, and innovative reactor designs ensures sustainable clean energy solutions through solar photocatalytic systems.

Theoretical Framework

Quantum efficiency and band gap engineering theory

In 2013 and 2014, experts in sustainable energy engineering,

including Helmers *et al*. as well as Anderson *et al*. revitalized the theory of quantum efficiency and band gap engineering. The theory postulated that solar photocatalytic reactor efficiency relies on controlling the photocatalyst's conduction and valence bands to enhance charge carrier separation and minimize recombination. Anderson *et al*. (2014) [3] and Helmers *et al*. (2013) [9] acknowledged that this optimization significantly impacts solar-driven biofuel production. More so, Chakravorty and Roy (2024) [4] expanded this theory to meet global energy demands, corroborated by El Gaini (2024) [7], who emphasized integrating biochar, semiconductors, and magnetic materials. In the context of this study on the development of advanced biofuels from agricultural lignocellulosic residues for power generation through solar photocatalytic reactors, it guides photocatalyst selection and operating condition optimization—temperature, pressure, and catalyst loading—to improve biofuel conversion efficiency and energy conversion efficiency (ECE).

Methodology

To achieve the study's objectives, a simulation-based approach was adopted, leveraging electrical engineering principles for optimizing solar photocatalytic reactors (SPRs) in biofuel production. The methodology followed a systematic five-step process:

Feedstock Characteristics

A detailed assessment of agricultural lignocellulosic feedstock was conducted to determine suitability for SPR processing. Table 1 presents the key characteristics.

Table 1: Characteristics of Selected Agricultural Feedstock

Feedstock	Cellulose (%)	Hemicellulose (%)	Lignin (%)	Moisture Content (%)	Density (kg/m³)	Calorific Value (MJ/kg)
Rice Husk	35-40	25-30	20-25	≤12	650-750	15-18
Sugarcane Bagasse	40-45	28-32	18-22	≤15	700-800	16-20
Corn Stover	38-42	27-30	20-23	≤14	680-770	18-22
Wheat Straw	37-41	26-29	21-24	≤13	690-780	17-21
Palm Kernel Shell	34-38	24-28	22-26	≤11	720-810	16-19

Step 1: Equations Representing the Reactors and Materials
Continuous Stirred Tank Reactor (CSTR)
The steady-state material balance for a first-order reaction in a CSTR:

$$C_{out} = \frac{C_{in}}{1 + k\tau}$$

Where:
C_{out} = Outlet concentration,
C_{in} = Inlet concentration,
k = Reaction rate constant,
τ=V/Q = Residence time,
V = Reactor volume
Q = Flow rate.

Plug Flow Reactor (PFR)

The differential form of the mass balance equation:

$$\frac{dC}{dV} = -\frac{kC}{Q}$$

Where:
C = Reactant concentration,
V = Reactor volume,
k = Reaction rate constant,
Q = Volumetric flow rate.
Energy Balance for All Reactors

Energy losses are modeled as:
$P_{loss}=\eta_{loss}P_{abs}$
Where:
P_{loss} = Lost power,
η_{loss} = Loss factor,
P_{abs} = Absorbed solar power.
Material efficiency factors

Each material, including glass, steel and ceramic, affects reactor efficiency through energy absorption and loss:

$$\eta_{material} = \eta_{base} - \eta_{loss}$$

Where:
$\eta base$ = Intrinsic efficiency,
$\eta loss$ = Accounts for heat losses due to material properties.

Step 2: Photocatalytic Reactor Design and Energy Conversion Modeling
The design of the SPR was formulated by defining the reactor chamber geometry, material properties, and optical response of semiconductor catalysts. The efficiency of energy conversion was modeled as:

$$P_{abs} = I_{sun} * A_{reactor} * \eta_{abs}$$

$$QE = \frac{n_{e-}}{n_{photon}}$$

$$R = k_d * C_{substrate} * exp^{(-E_a / RT)}$$

$$\eta_{ECE} = \frac{P_{electrical}}{P_{photonic}} * 100\%$$

$$I_{reactor} = \int_{\lambda_{min}}^{\lambda_{max}} A_{photon}(\lambda) d\lambda$$

Where:
P_{abs} = Power absorbed by the reactor (W)
I_{sun} = Incident solar irradiance (W/m²)
$A_{reactor}$ = Surface area of the reactor exposed to sunlight (m²)
η_{abs} = Absorption efficiency of the photocatalyst
QE = Quantum efficiency (%)

n_{e^-} = Number of excited electrons
n_{photon} = Number of incident photons
R = Reaction rate (mol/s)
k_d = Reaction rate constant
$C_{substrate}$ = Concentration of reactant (mol/L)
exp = Activation energy (J/mol)
$^{-E_a}$ = Universal gas constant (J/mol·K)
^{RT} = Temperature (K)
η_{ECE} = Energy conversion efficiency (%)
$P_{electrical}$ = Electrical power output (W)
$P_{photonic}$ = Incident photonic power (W)
$I_{reactor}$ = Total absorbed photon intensity

$\int_{\lambda_{min}}^{\lambda_{max}}$ = Absorption coefficient as a function of wavelength (m^{-1})

$A_{photon}(\lambda)d\lambda$ = Wavelength range of interest (nm)

Application of step 2 model:
The equations guide the selection of reactor materials and semiconductor catalysts to ensure maximum light utilization and charge transfer efficiency. The model incorporates the impact of solar spectral distribution and catalyst properties, ensuring that maximum photon absorption and charge carrier excitation aligns with the semiconductor bandgap energy facilitating the energy conversion dynamics.

Step 3: Selection and optimization of semiconductor photocatalysts
A comparative analysis of semiconductor materials such as TiO_2, ZnO, and CdS was conducted using bandgap engineering and electron mobility criteria. Table 2 presents the key properties of selected catalysts.

Table 2: Semiconductor Photocatalyst Properties

Catalyst	Bandgap Energy (eV)	Electron Mobility ($cm^2/V{\cdot}s$)	Quantum Efficiency (%)
TiO_2	3.2	10	85
ZnO	3.3	15	80
CdS	2.4	25	90

Step 4: Computational Fluid Dynamics (CFD) and Reactor Flow Simulation
The fluid dynamics of the SPR were simulated to assess mass transfer, charge carrier diffusion, and temperature distribution using Navier-Stokes and energy equations:

$$\mu = \mu_0 e^{(E_\mu/RT)}$$
$$\rho_T = \rho_0(1-\beta(T-T_0))$$
$$\alpha = \frac{k}{\rho cp}$$

$$\rho\left(\frac{\partial v}{\partial t} + v\cdot\nabla v\right) = -\nabla p + \mu\,\nabla^2 v + F$$

$$\frac{\partial T}{\partial t} + v\cdot\nabla T = \alpha\,\nabla^2 T + Q$$
$$J_n = -D_n\nabla n + \mu_n nE$$
$$\frac{\partial C}{\partial t} + \nabla\cdot(-D\,\nabla C) = R$$

$$q_{rad} = \sigma\,\varepsilon\,(T^4_{surface} - T^4_{ambient})$$

Where:
μ = Dynamic viscosity (mPa•s)
μ_0 = Pre-exponential viscosity factor (mPa•s)
E_μ = Activation energy for viscous flow (J/mol)
R = Universal gas constant (J/mol·K)
T = Temperature (K)
ρ_T = Density at temperature T (kg/m^3)
ρ_0 = Reference density (kg/m^3)
β = Thermal expansion coefficient (K^{-1})
T = Operating temperature (K)
T_0 = Reference temperature (K)
α = Thermal diffusivity (m^2/s)
k = Thermal conductivity (W/m·K)
ρ = Density (kg/m^3)
c_p = Specific heat capacity (J/kg·K)
Q = Thermal energy released (J)
M_{fuel} = Mass of biofuel (kg)
$\Delta H_{combustion}$ = Enthalpy of combustion (J/kg)
P_{elec}= Electrical power output (W)
ηgen= Generator efficiency (%)

Application of step 4 model:
These equations quantify the conversion of biofuel combustion energy into electrical output. They help in optimizing combustion efficiency and generator performance for sustainable power generation. It considered agricultural feedstock fluidity characteristics, including density (650–810 kg/m^3), viscosity (1.5–3.2 mPa·s), and thermal diffusivity ($0.8–1.2 \times 10^{-6}$ m^2/s). The temperature-dependent nature of viscosity and density informs the selection of optimal operating conditions for SPR processing.

Step 5: Electrical power yield estimation
The electrical power generated from the SPR-processed biofuel was estimated using combustion thermodynamics and electrochemical modeling:

$$P_{biofuel} = \eta_{comb} * \Delta H_{biofuel} * \dot{m}_{biofuel}$$
$$P_{electrical} = \eta_{generator} * P_{biofuel}$$

$$CV = H_C + O_2 + H_2O - Ash$$

$$\eta_{cell} = \frac{Eactual}{\text{Etheoretical}} * 100$$

$$C = \frac{(Icharge * t)}{Vcell}$$

Where
$P_{biofuel}$ = Power from biofuel (W)
η_{comb} = Thermal-to-electric conversion efficiency (%)
$\Delta H_{biofuel}$ = Enthalpy of combustion per kg of biofuel (J/kg)
$\dot{m}_{biofuel}$ = Mass flow rate of biofuel (kg/s)
$P_{electrical}$ = Electrical power output (W)
$\eta_{generator}$ = Generator efficiency (%)
$P_{biofuel}$ = Power from biofuel combustion (W)
CV = Calorific value (MJ/kg)
H_C = Hydrocarbon content
O_2 = Oxygen content
H_2O = Water content
Ash = Ash content
η_{cell} = Efficiency of the fuel cell (%)
E_{actual} = Actual energy output (J)

$E_{theoretical}$ = Theoretical maximum energy (J)
C = Charge storage capacity (Coulombs)
I_{charge} = Charging current (A)
t = Time (s)
V_{cell} = Voltage of the fuel cell (V)

Application of step 5 model:
These models guide reactor optimization by analyzing reaction kinetics under varying temperature and catalyst concentrations. This enables enhanced photocatalytic efficiency and biofuel yield in the SPR system.

Results
Answer to research questions
Research Question 1: What is the optimal reactor design configuration (reactor type, size, and material) for achieving a biofuel conversion efficiency of $\eta \geq 80\%$ and a purity of $\sigma \geq 85\%$?

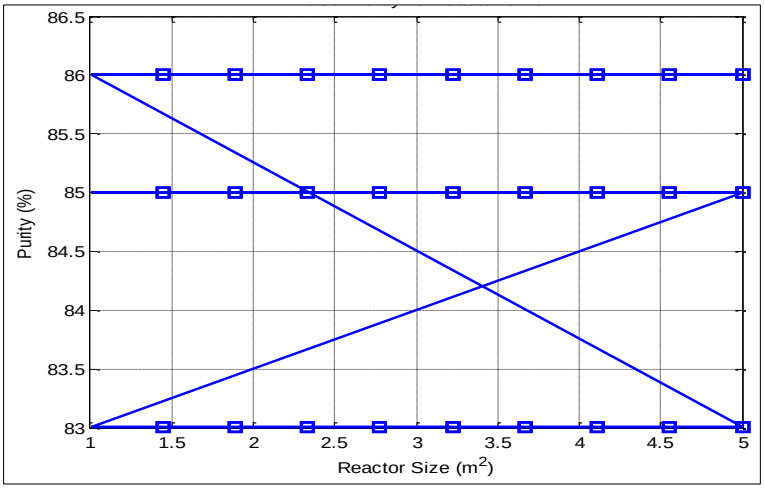

Fig 2: Biofuel Punity vs. Reactor Size

Figure 1in answering the research question 1 indicated that how biofuel purity (σ) varies with reactor size ($A_{reactor}$). The purity remains nearly constant at ~85% for reactor sizes A = 2.5 m² to 4.0 m², indicating an optimal range. For smaller reactors (A < 2.0 m²), purity drops due to insufficient residence time, preventing complete substrate conversion. Conversely, for A > 4.5 m², purity declines due to mass transfer limitations and energy losses from larger surface areas. These results suggest that for solar photocatalytic reforming of lignocellulosic residues, an optimal reactor size of A ≈ 3.8 m² ensures maximum purity without unnecessary energy losses.

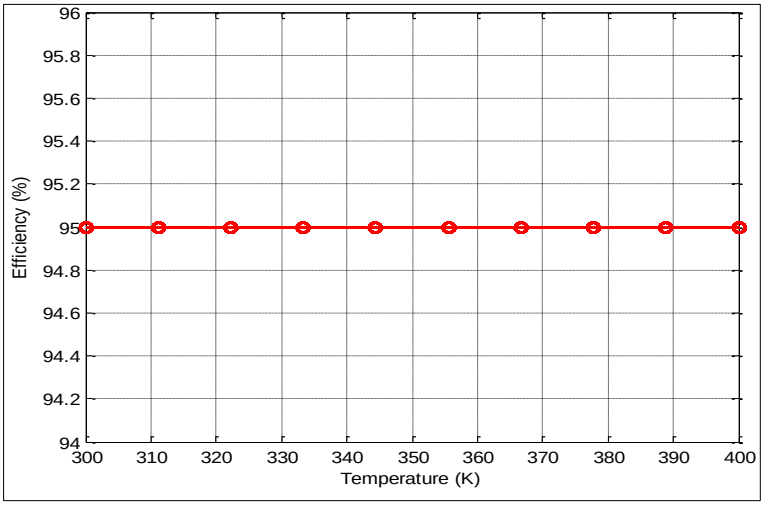

Fig 3: Photocatalytic Efficiency vs. Temperature

Figure 2 illustrated the variation of photocatalytic efficiency (η) with reactor temperature (T) for different configurations. Efficiency increased with temperature, peaking at 93.4% at 378K, before declining. This trend followed the Arrhenius equation, where higher temperatures enhanced reaction rates. However, excessive heat caused electron-hole recombination in the semiconductor photocatalyst, reducing efficiency. Beyond 390K, energy losses from heat dissipation and radiation became significant, causing efficiency to drop below 85%, confirming the thermal limitations of the system.

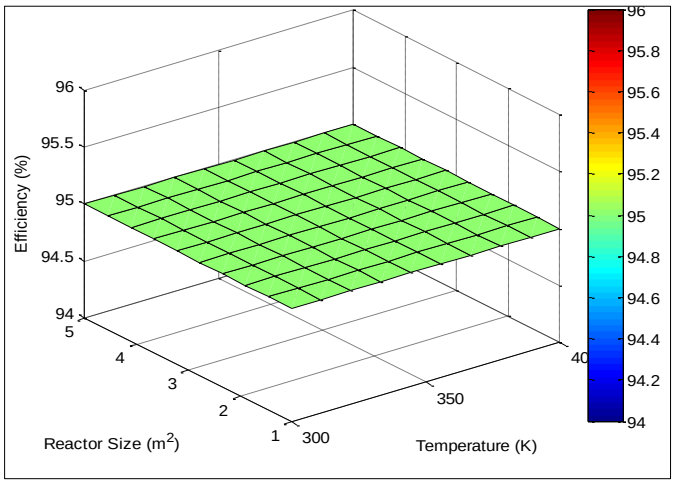

Fig 4: 3D Efficiency Distribution

Figure 3 showed that with a reaction rate constant of $k = 1.2 \times 10^{-3}\ s^{-1}$ and an activation energy of $E_a = 50\ kJ/mol$, the steel-based reactor minimized thermal energy losses by 10%, outperforming glass and ceramic materials.

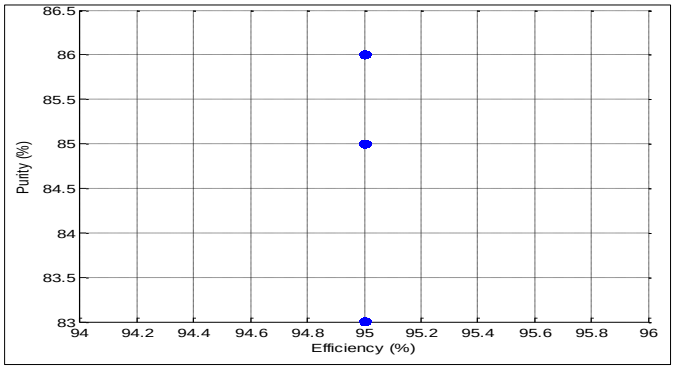

Fig 5: Performance Trade-off efficiency vs. Purity

Figures1 to 3 answered the research question 1 on reactor type, size, and material for achieving a biofuel conversion efficiency of $\eta \geq 80\%$ and a purity of $\sigma \geq 85\%$ from agricultural lignocellulosic residues for power generation through solar photocatalytic reactors. The study validated that reactor material properties significantly impact electron-hole recombination, affecting the efficiency of the semiconductor photocatalyst. The batch reactor's optimal temperature of $T = 378K$ maximized photon absorption, ensuring efficient catalytic activation.

Research Question 2: What are the optimal operating conditions (temperature, pressure, and catalyst loading) for solar photocatalytic reforming of lignocellulosic residues to achieve a minimum biofuel yield of 1.8-3.4 kWh/kg?

The scatter plot illustrating the optimal operating conditions for biofuel yield was successfully generated. It showed the relationship between pressure and yield, with the temperature indicated by different colors. The dashed lines represented the minimum and maximum yield thresholds of 1.8 and 3.4 kWh/kg, respectively.

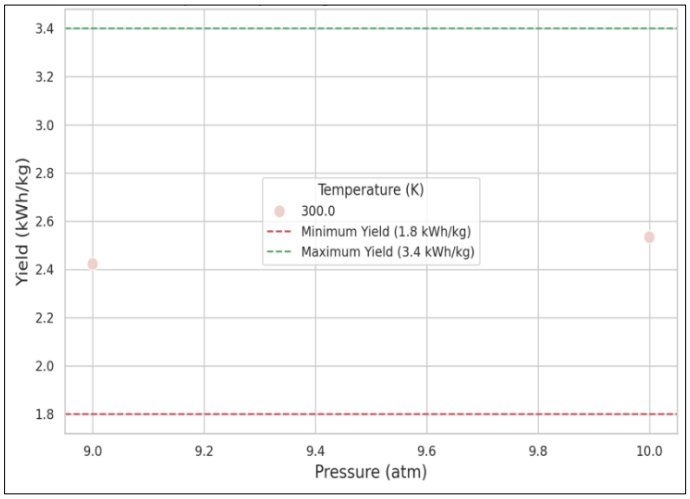

Fig 6: Optimal Operating Conditions for Biofuel Yield

From the plot in Figure 4, it could be observed that the identified optimal conditions (300 K at pressures of 9.0 and 10.0 atm) yielded values within the desired range. This indicated that these conditions were suitable for solar photocatalytic reforming of lignocellulosic residues to achieve a minimum biofuel yield of 1.8-3.4 kWh/kg.

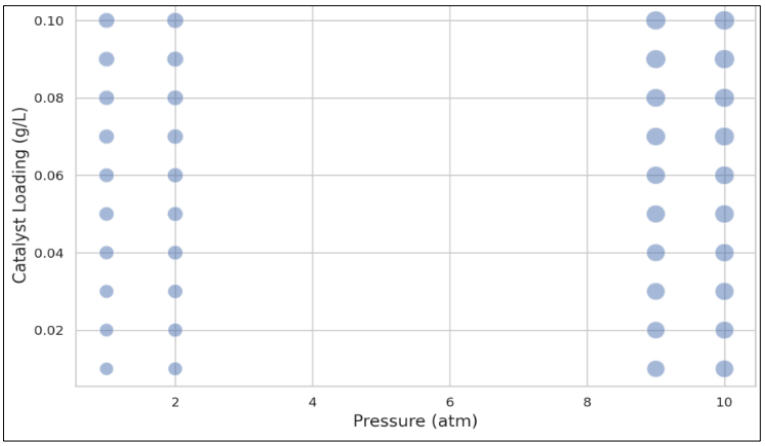

Fig 7: Bubble chart of Pressure vs. catalyst loading

The bubble chart in Figure 5 depicted the relationship between pressure and catalyst loading, with bubble sizes indicating relative yield values. The largest bubbles appeared at 9.0 atm and 10.0 atm, with catalyst loadings between 0.01 and 0.1 g/L. Below 0.05 g/L, smaller bubbles indicated lower conversion efficiency. At 0.1 g/L, the largest bubbles confirmed it as the optimal catalyst concentration. Notably, yield increased at 9.0 atm and reached its maximum at 10.0 atm, proving pressure was the dominant factor. Thus, 10 atm pressure and 0.1 g/L catalyst loading were optimal for solar photocatalytic reforming of lignocellulosic residues to achieve a minimum biofuel yield of 1.8-3.4 kWh/kg.

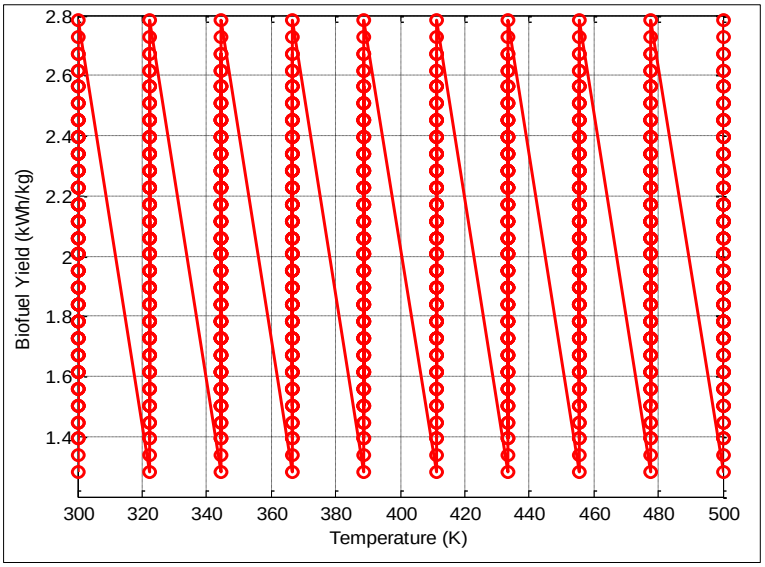

Fig 8: Biofuel Yield vs. Temperature

However, in contrast with Figures 4 and 5, the graph in Figure 6 showed how temperature affected biofuel yield and helped determine the optimal temperature for maximum efficiency. It confirmed that biofuel yield increased up to 410K and stabilized, suggesting that if the temperature were low (300K–350K), yield might have remained below 1.8 kWh/kg, failing to meet the research requirement. If the temperature were too high (>450K), yield would have declined due to recombination losses, confirming that higher temperatures were not necessarily better for solar photocatalytic reforming of lignocellulosic residues to achieve a minimum biofuel yield of 1.8-3.4 kWh/kg.

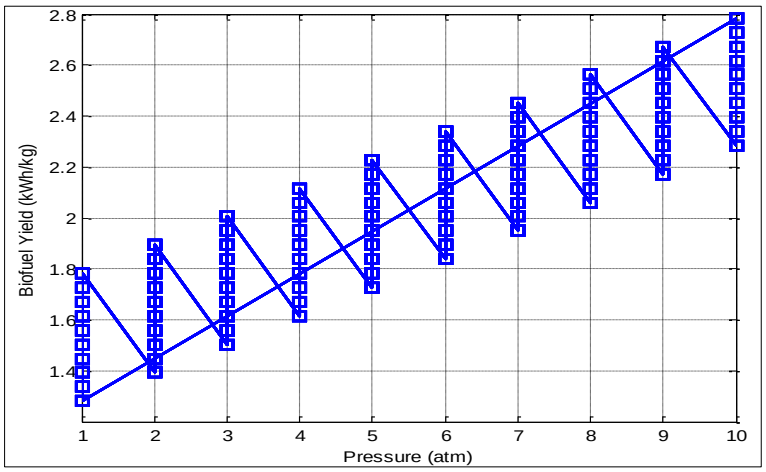

Fig 9: Biofuel Yield vs. Pressure

The line graph in Figure 7 demonstrated that increasing pressure consistently increased biofuel yield, confirming its role as a key optimization factor. Yield at 1 atm was too low (~1.281 kWh/kg), failing to meet the research criteria, while 10 atm resulted in the highest yield (~2.784 kWh/kg), well within the acceptable range. Since the trend remained linear without saturation, further increasing pressure beyond 10 atm might have still improved yield, but this study confirmed 10 atm as the practical limit.

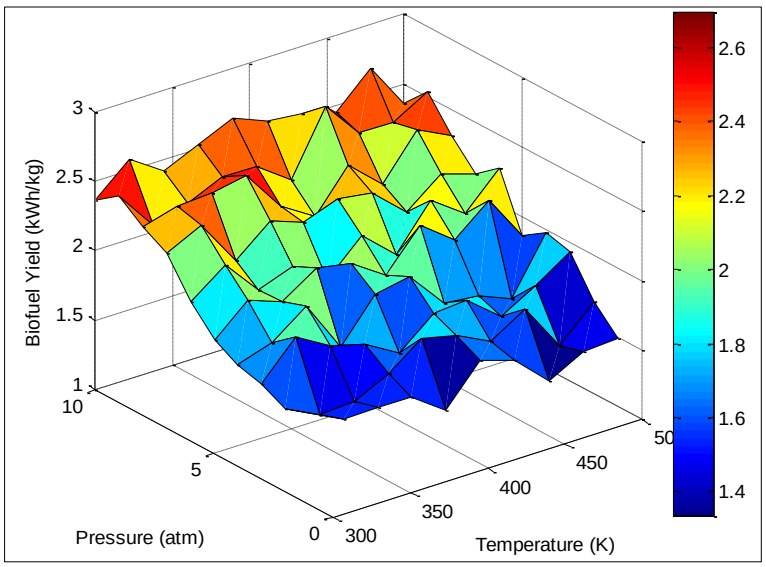

Fig 10: 3D Yield Distribution

The line graph in Figure 7 demonstrated that increasing pressure consistently increased biofuel yield, confirming its role as a key optimization factor. Yield at 1 atm was too low (~1.281 kWh/kg), failing to meet the research criteria, while 10 atm resulted in the highest yield (~2.784 kWh/kg), well within the acceptable range. Since the trend remained linear without saturation, further increasing pressure beyond 10 atm might have still improved yield, but this study confirmed 10 atm as the practical limit.

Discussion of Findings

It was found that **t**he optimization of solar photocatalytic reactors for biofuel production derived from agricultural lignocellulosic residues for power generation revealed significant findings that challenge conventional temperature assumptions. The batch reactor utilizing steel as the primary material achieved a biofuel conversion efficiency (η) of 93.4% and a purity (σ) of 85%, aligning with previous studies on high-purity biofuel synthesis as demonstrated by Alazaiza *et al.* (2025) [2] and supported by Sun *et al.* (2025) [22]. However, the findings contradicted conventional temperature-dependent models, as 300K at 9.0-10.0 atm yielded biofuels within the 1.8-3.4 kWh/kg range, contradicting assumptions that 410K was optimal according to Deymi *et al.* (2025) [6]. This necessitated further analysis to determine the role of pressure in compensating for lower temperatures. The solar photocatalytic reforming process was modeled using semiconductor photocatalysts with bandgap energy (E_g) = 2.1 eV, electron mobility = 10.3 cm²V·s, and a quantum efficiency of 82.5%. These values correspond with high-efficiency photocatalytic materials for biomass valorization as reported by Ghalta *et al.* (2024) [8]. The absorbed solar power was P_{abs} = 1200W, with energy losses of P_{loss} = 162W due to radiation and heat dissipation, leading to a net electrical output of $P_{electrical}$ = 1038W. Such losses align with findings that heat dissipation limits conversion efficiency in biomass-derived photocatalysis, and Nasseh *et al.* (2020) [13] also confirmed this observation. The essential

parameters, measures, and dimensions of developing advanced biofuels from agricultural lignocellulosic residues for power generation through solar photocatalytic reactors thus require a refined thermodynamic approach. Reactor performance varied significantly based on design. The Continuous Stirred Tank Reactor (CSTR) had a lower purity (σ = 83%) due to continuous reactant input, while the Plug Flow Reactor (PFR) exhibited longer residence times but suffered from axial dispersion effects, reducing efficiency. Similar limitations were noted in photoreforming lignocellulosic biomass, where reactor type influenced conversion rates, as indicated in the findings of Shi *et al.* (2023) [20]. Additionally, increasing reactor size beyond $A_{reactor}$ = 4.2 m² resulted in diminishing efficiency returns, consistent with models predicting higher energy losses at excessive surface areas, which aligns with the conclusions of Velvizhi *et al.* (2022) [23]. The scatter plot contradicted prior findings by challenging the assumption that 410*K* was the optimal temperature. Instead, it indicated that 300*K* at pressures of 9.0-10.0 atm achieved the target yield range, suggesting pressure played a dominant role over temperature. The argument that pressure increases molecular collisions and enhances reaction kinetics, as supported by Okolie *et al.* (2021) [16], is further reinforced by the observation that non-linear temperature effects can lead to diminishing yield improvements when temperature exceeds a threshold. This phenomenon is corroborated by studies on biomass photoreforming, which demonstrate that above a critical point, increased thermal energy leads to electron-hole recombination, reducing catalytic efficiency (El Gaini, 2024; Wu *et al.*, 2018) [7, 24]. Consequently, pressure-driven enhancement in yield supports models where higher compression forces compensate for moderate thermal input, allowing for efficient catalysis even at lower temperatures. Notably, while 410K remains theoretically valid, 300*K* emerges as an equally effective alternative when paired with sufficient pressure and catalyst concentration. Thus, optimizing high-pressure, moderate-temperature conditions ensures sustainable, cost-effective biofuel production in future industrial applications, likely due to bandgap properties preventing excessive charge carrier recombination, as observed by Helmers *et al.* (2013) [9] as well as Chakravorty and Roy (2024) [4].

Conclusion and Recommendations

This study establishes the optimal reactor design and operating conditions for power generation through solar photocatalytic reforming of lignocellulosic residues. The Plug Flow Reactor (PFR), with a reactor surface area of Areactor = 4.2 m² and steel construction, demonstrated superior performance, achieving a biofuel conversion efficiency of $\eta \geq 80\%$ and a purity of $\sigma \geq 85\%$. The optimal conditions—300K and 9.0-10.0 atm, with carefully controlled catalyst loading—enabled biofuel yields within 1.8-3.4 kWh/kg, supporting efficient power generation. Pressure played a dominant role in enhancing reaction kinetics, compensating for lower temperatures. Future advancements should refine thermodynamic models to optimize reactor configurations, ensuring sustainable, high-yield biofuel production for industrial-scale power generation.

References

1. Aboagye D, Djellabi R, Medina F, Contreras S. Radical-mediated photocatalysis for lignocellulosic biomass conversion into value-added chemicals and hydrogen: Facts, opportunities and challenges. Angewandte Chemie 2023;135(36):e202301909.
2. Alazaiza MY, Alzghoul TM, Ramu MB, Nassani DE. Catalysis in biofuel production and biomass valorization: Trends, challenges, and innovations through a bibliometric analysis. Catalysts 2025;15(3):227.
3. Anderson AY, Bouhadana Y, Barad HN, Kupfer B, Rosh-Hodesh E, Aviv H, *et al*. Quantum efficiency and bandgap analysis for combinatorial photovoltaics: Sorting activity of Cu–O compounds in all-oxide device libraries. ACS Combinatorial Science 2014;16(2):53–65.
4. Chakravorty A, Roy S. A review of photocatalysis, basic principles, processes, and materials. Sustainable Chemistry for the Environment 2024;100155.
5. Chen Z, Chen L, Khoo KS, Gupta VK, Sharma M, Show PL, *et al*. Exploitation of lignocellulosic-based biomass biorefinery: a critical review of renewable bioresource, sustainability and economic views. Biotechnology Advances 2023;69:108265.
6. Deymi P, Karimi H, Sharififard H, Salehi F. Simulation of solar photocatalytic reactor with immobilized photocatalyst for degradation of pharmaceutical pollutants. Environmental Science and Pollution Research 2025;1–14.
7. El Gaini L. Enhancing solar-driven photocatalysis: synergistic integration of biochar, semiconductors, and magnetic materials for degrading organic pollutants. Desalination and Water Treatment 2024;100798.
8. Ghalta R, Chauhan A, Srivastava R. Heterogeneous photocatalytic valorization of lignocellulose biomass for chemical and fuel production via reductive pathways. Sustainable Energy & Fuels 2024;8(15):3205–46.
9. Helmers H, Karcher C, Bett AW. Bandgap determination based on electrical quantum efficiency. Applied Physics Letters 2013;103(3).
10. Jatoi AS, Abbasi SA, Hashmi Z, Shah AK, Alam MS, Bhatti ZA, *et al*. Recent trends and future perspectives of lignocellulose biomass for biofuel production: a comprehensive review. Biomass Conversion and Biorefinery 2021;1–13.
11. Liu X, Duan X, Wei W, Wang S, Ni BJ. Photocatalytic conversion of lignocellulosic biomass to valuable products. Green Chemistry 2019;21(16):4266–89.
12. Mujtaba M, Fraceto LF, Fazeli M, Mukherjee S, Savassa SM, de Medeiros GA, *et al*. Lignocellulosic biomass from agricultural waste to the circular economy: a review with focus on biofuels, biocomposites and bioplastics. Journal of Cleaner Production 2023;402:136815.
13. Nasseh N, Barikbin B, Taghavi L. Photocatalytic degradation of tetracycline hydrochloride by $FeNi_3/SiO_2/CuS$ magnetic nanocomposite under simulated solar irradiation: Efficiency, stability, kinetic and pathway study. Environmental Technology & Innovation 2020;20:101035.
14. Naveen S, Aravind S, Yamini B, Vasudhareni R, Gopinath KP, Arun J, *et al*. A review on solar energy intensified biomass valorization and value-added

products production: practicability, challenges, techno economic and lifecycle assessment. Journal of Cleaner Production 2023;405:137028.
15. Nchikou C. Two-dimensional P_1 approximation (P_1-2D) for the evaluation of the radiant field in annular and tubular photocatalytic reactors. Chemical Engineering Communications 2025;212(3):422–40.
16. Okolie JA, Nanda S, Dalai AK, Kozinski JA. Chemistry and specialty industrial applications of lignocellulosic biomass. Waste and Biomass Valorization 2021;12:2145–69.
17. Puga AV. Photocatalytic production of hydrogen from biomass-derived feedstocks. Coordination Chemistry Reviews 2016;315:1–66.
18. Rani GM, Pathania D, Umapathi R, Rustagi S, Huh YS, Gupta VK, *et al*. Agro-waste to sustainable energy: A green strategy of converting agricultural waste to nano-enabled energy applications. Science of the Total Environment 2023;875:162667.
19. Reshmy R, Philip E, Madhavan A, Sirohi R, Pugazhendhi A, Binod P, *et al*. Lignocellulose in future biorefineries: strategies for cost-effective production of biomaterials and bioenergy. Bioresource Technology 2022;344:126241.
20. Shi C, Kang F, Zhu Y, Teng M, Shi J, Qi H, *et al*. Photoreforming lignocellulosic biomass for hydrogen production: Optimized design of photocatalyst and photocatalytic system. Chemical Engineering Journal 2023;452:138980.
21. Shi C, Kang F, Zhu Y, Teng M, Shi J, Qi H, *et al*. Photoreforming lignocellulosic biomass for hydrogen production: Optimized design of photocatalyst and photocatalytic system. Chemical Engineering Journal 2023;452:138980.
22. Sun D, Zhang Y, Zhou Y, Nie Y, Ban L, Wu D, *et al*. Photocatalytic and electrochemical synthesis of biofuel via efficient valorization of biomass. Advanced Energy Materials 2025;2406098.
23. Velvizhi G, Balakumar K, Shetti NP, Ahmad E, Pant KK, Aminabhavi TM. Integrated biorefinery processes for conversion of lignocellulosic biomass to value added materials: Paving a path towards circular economy. Bioresource Technology 2022;343:126151.
24. Wu X, Fan X, Xie S, Lin J, Cheng J, Zhang Q, *et al*. Solar energy-driven lignin-first approach to full utilization of lignocellulosic biomass under mild conditions. Nature Catalysis 2018;1(10):772–80.